Moroccan Journal of Chemistry
ISSN: 2351-812X
http://revues.imist.ma/?journal=morjchem&page=login
E. Mourid & al. / Mor. J. Chem. 9 N°1 (2021) 028-043

Water reuse after removing a textile dye methyl orange using a recyclable hydrotalcite material

E. Mourid, M. Lakraimi*, L. Benaziz, M. Cherkaoui

Physical Chemistry of Materials Team, Cadi Ayyad University, Marrakech, Morocco

** Corresponding author:*
mlakraimi@yahoo.fr
Received 31 May 2020,
Revised 23 Sep 2020,
Accepted 06 Nov 2020

Abstract

Hydrotalcite type material based on zinc, aluminum and carbonates was synthesized by coprecipitation method and its derived calcined at 500°C (CHT) was used to remove the textile dye methyl orange (MO). This adsorbent has a great potential for removing pollutants from aqueous solutions without generating sludge. Adsorption was performed in batch experiments. A rapid process of retention confirmed by kinetics reflects a high affinity between CHT material and MO dye. The adsorption isotherms follow the Langmuir model (L type). The results of several techniques suggest the intercalation of the pollutant between the hydrotacite sheets reconstructed from mixed oxides with a gallery of 2.35 nm. The retention capacity reaches 2500 mg/g with a removal rate of 100% for an optimum mass ratio MO/CHT of 0.3. After the recycling studies the material CHT justify its recyclability and confirms its efficiency for eliminating such pollutant.

Keywords: *Calcined hydrotalcite; Textile dye MO; Wastewater treatment; Efficiency; Recycling.*

1. Introduction

The manufacturing sector is considered an index of economic growth in several countries; unfortunately, it generates various categories of waste that infect the environment and human health. By way of example, the textile sector is responsible for releases laden with highly toxic and non-biodegradable dyes, which is consist of azo compounds (-N=N-) and their derivatives with benzene molecules. Among the azo compounds commonly used, we can mention the methyl orange (MO), which is considered a carcinogenic and mutagenic compound [1-2]. Nowadays, pollution has become a major global problem due to a lack of preliminary treatment of industrial waste before landing in nature and the use of efficient methods that does not generate sludge [3]. The protection of the environment has thus become a major economic and political issue. Adsorption is one of the most used processes to remove the pollutants by the materials such as calcium phosphates, natural phosphate, clays, activated carbon, natural serpentine, etc. [4-10]. Some used adsorbents have a low cost and do not generate sludge [11-14]. The adsorption method eliminates the color with optimization of a few influencing parameters, it is not expensive and do not lead to the production of other secondary products. Therefore, contaminated water discharges are considered a problem for textile industries. Adsorption on adsorbent materials remains among the most used techniques in wastewater treatment and easy to implement. The adsorption of organic molecules such as those of the dyes on the calcined hydrotalcite has proved to be a very effective treatment technique and does not generate discharges [15]. Mixed oxides from calcined hydrotalcites retain the property of reconstructing the initial hydrotacite phases, thus promoting the retention of several toxic pollutants in their anionic forms [1, 16, 17]. In the present study, the retention of the anionic dye by calcined hydrotalcite forming an organic-inorganic nanohybrid composite was reported and discussed. The influence of contact time, solution pH and the mass ratio adsorbate/adsorbent on the adsorption process was investigated. The localization of the azo dye MO in the interlamellar space of the reconstructed hydrotalcite was studied by X-ray diffraction that allows us to determine the apparent interlamellar distance of reconstructed anionic clay material. Finally, the results of other characterization techniques used, such as infrared spectroscopy and scanning electron microscopy were discussed in order to confirm the elimination of the MO dye and therefore the efficiency of the chosen material.

2. Experimental

2.1. Adsorbate compound

The MO dye is a mono-azo dye characterized by the azo chromophore (-N=N-). It is purchased from Sigma-Aldrich, ACS reagent, it is a colored indicator (Heliantine) and used mainly for printing and coloring textiles. Some of the important chemical and physical properties of the azo dye MO are listed in Table 1.

2.2. Toxicology

A study carried out on the overlap of the LD50 (median lethal dose) with the chemical and dye classifications of dyes, shows that the most toxic are generally the azo and cationic dyes [1]. However, the electro-attracting nature of the azo groups generates electronic deficiencies, which makes azo compounds unwilling to oxidative catabolism under aerobic environmental conditions. The toxicity of azoics from exposure to dyes and their metabolites is not new. Since 1895, the increase in the number of bladder cancers observed in textile workers was linked to their prolonged exposure to azo dyes. Since then, the work on these dyes has demonstrated that these chemical compounds have carcinogenic effects on humans and animals [18-20].The carcinogenic impact of this compound is expressed indirectly by their amino derivatives. The bond of the azo compound can easily break under the enzymatic action (enzyme azo-reductase P 450) to transforme into a carcinogenic amino compound [21].

Table 1: Chemical and physical properties of the chosen pollutant

Trade name	Methyl orange
Systematic name	4-dimethylaminoazobenzene-4-sulfate
Class	Azo
Chemical structure	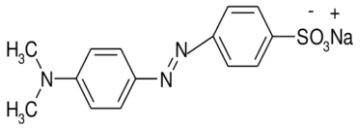
Formula	$C_{14}H_{14}N_3NaO_3S$
Molecular weight	327.33 g/mol
Solubility in water	5.2 g/L at 20 °C
LD50	60 mg/kg
pK_a	3.39
Density	1.28 g/cm^3

2.3. Preparation of the adsorbent material

The hydrotalcite material based in Zn-Al intercalated by carbonate anions was synthesized by coprecipitaion method at pH 10 from a mixture of metal salts $AlCl_3.6H_2O$ (99% of purity) 0.5M and $Zn(SO_4).7H_2O$ (99% of purity) 0.5M with a metal ratio Zn/Al = 2. The pH was maintained at 10 by adding a solution of basic anions containing 0.75M of Na_2CO_3 (99% of purity) and 0.25M of NaOH (98% of purity), the chemicals were purchased from Sigma-Aldrich. At the end of the precipitation reaction, a maturation time of 72 hours with moderate stirring was adopted, and then the anionic clay material obtained was calcined at 500 °C for 5 hours.

2.4. Retention experiments

The solutions of the dye MO are prepared in a range of concentrations from 30 to 1000 mg/L, the dilution is carried out in Erlenmeyer flasks (100 mL). The quantity (Q) of MO retained by CHT was calculated by the difference between the initial (C_i) and the equilibrium (C_e) concentrations of the dye solution in a volume of solution (V) using a mass of the adsorbent (m) according to the below formula:

$$Q = (C_i - C_e) \times V/m \quad (1)$$

For the thermodynamic study, the same adsorption process was followed under optimal conditions as a function of time in a thermostatic bath, in order to regulate the desired temperature.

2.5. Characterization techniques

After the retention of the pollutant by the CHT material, the residual concentration of MO was evaluated by a Jenway-6300 UV/Vis spectrophotometer in the visible range. The characteristic bands are identified using infrared spectroscopy with a JASCO FT/IR-4600 model at a resolution of 2 cm^{-1} and on average over 100 scans. The morphology was visualized by SEM scanning electron microscopy coupled by EDX analysis performed by TESCAN VEGA 3 LM/EDAX, with a magnification of 10.000 times and a voltage of 10 kV. The phases obtained are identified by X-ray diffraction with an XPERT-PRO powder diffractometer equipped with a Cu anticathode whose Kα radiation has a wavelength λ = 0.15415 nm; the angular range is from 2-70° and the step of counting time is 41s.

3. Results and discussion

3.1. Characterization of the CHT material

From Figure 1a, the obtained phase is comparable to that of natural hydrotalcite [22], it confirms the existence of a best crystallized HT phase, and the lines observed are indexed in a hexagonal system of rhombohedral symmetry, with a space group $R\bar{3}m$. The cell parameters identified are, d = 0.764 nm represents the lamellar distance, 0.306 nm for (a) parameter and 2.292 nm for (c) parameter. The IR spectrum (Figure 1b) of HT shows the characteristic bands of the interlayer water molecules δ (H_2O) and vibrations bands of the hydroxyl group ν (O-H). Furthermore, the characteristic bands of carbonate anions are between 879 and 1480 cm^{-1}. The band observed at 554 cm^{-1} corresponds to Al-O and another at 615 cm^{-1} to Zn-O [23]. The band that appears around 400 cm^{-1} corresponds to O-M-O vibrations [24]. The SEM photographs are presented in Figure 1c for the HT phase, it can be noted the appearance of the lamellar structure with the presence of crystallites in the form of a sand rose. For the calcined phase (Figure 1d), it can be remarked an absence of the lamellar character involve the destruction of the HT sheets. Figure 1e shows the EDX analysis of the HT compound. This analysis shows the appearance of elements existing in the HT material such as zinc, aluminum, oxygen and carbon.

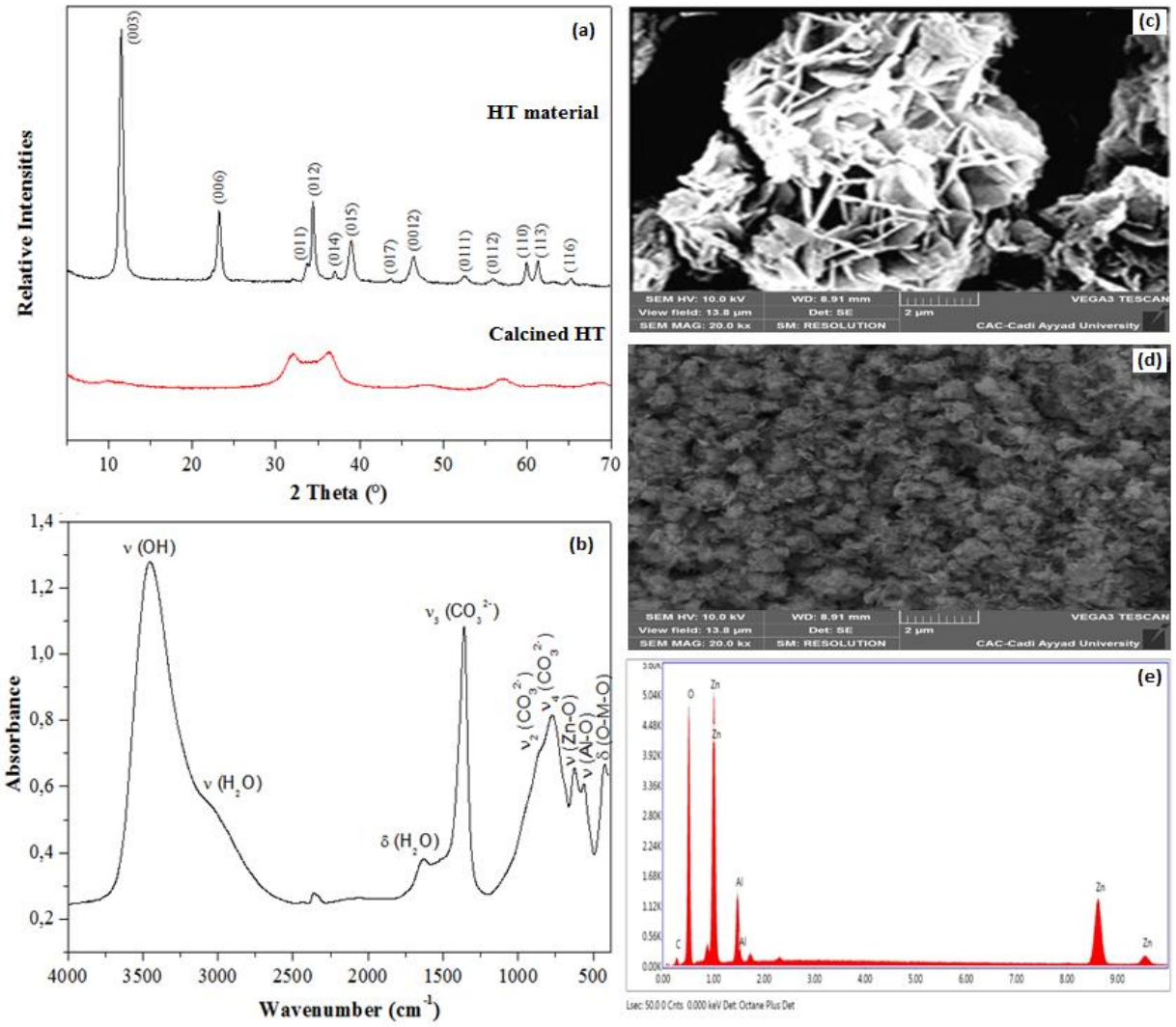

Figure 1: XRD patterns of HT and CHT (a), IR spectrum of HT (b), SEM photographs of HT (c) and CHT (d), and EDX analysis of HT (e)

3.2. Effect of pH

The influence of pH on the reconstruction phenomenon was investigated using 30 mg of CHT and an initial concentration of MO in solution of 50 mg/L. Subsequently, the suspensions were adjusted to pH values between 4 and 10.The results of the retention of MO by CHT as a function of pH are shown in Figure 2. The decrease retention amounts in acidic and basic mediums can be attributed to partial dissolution of the material or by protonation of the dye and the competition with anions CO_3^{2-} [25]. The maximum retention is obtained for pH value of 6.

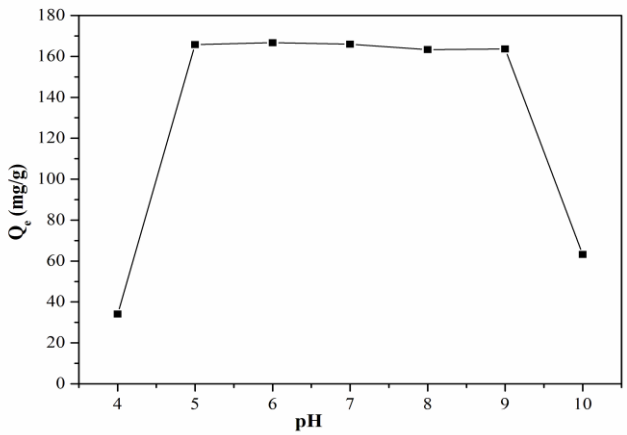

Figure 2: Amounts of MO retained by CHT at different pH values (m_{CHT} = 30 mg, [MO] = 50 mg/L, t_c = 120 min)

3.3. Effect of contact time

The evolution of the amount of MO retained by 50 mg of CHT, as a function of the contact time (15 - 180 min) for initial MO concentrations of 50, 200 and 800 mg/L is shown in Figure 3. The adsorption of MO by CHT is rapid, due to the strong interactions between the surface of the adsorbent and the pollutant [26], and progresses to reach saturation of the material sites. The equilibrium is reached after 15 min for a concentration of 50 mg/L, after 30 min for 200 mg/L and after 60 min of agitation for MO concentration of 800 mg/L.

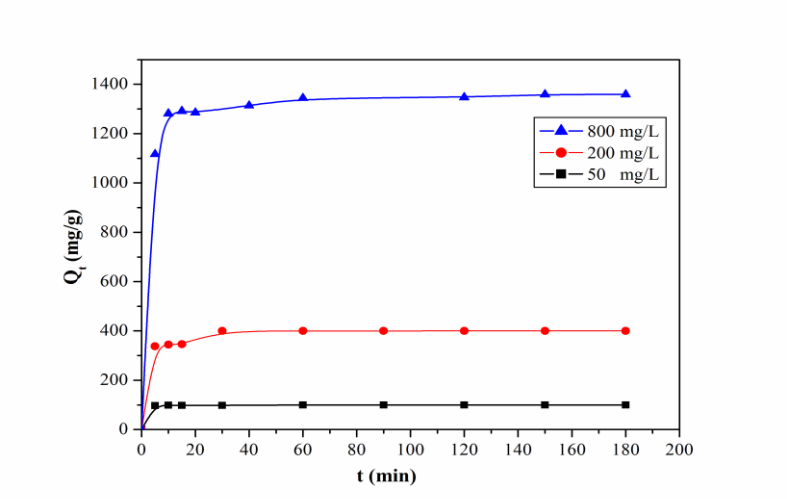

Figure 3: Kinetics of MO adsorption by 50 mg of CHT at three different concentrations

3.4. Kinetic model

In order to describe the kinetic behavior during the retention of the studied dye, two models were explored, the pseudo-first order and the pseudo-second order models. The first model gave correlation coefficients too far from

unity. The results are described by the pseudo-second order model, its kinetic parameters are presented in Figure 4, and the linear transformation of this model is expressed by Equation (2):

$$t/Q_t = (1/Q_e)\times t + 1/(k_2 Q_e^2) \quad (2)$$

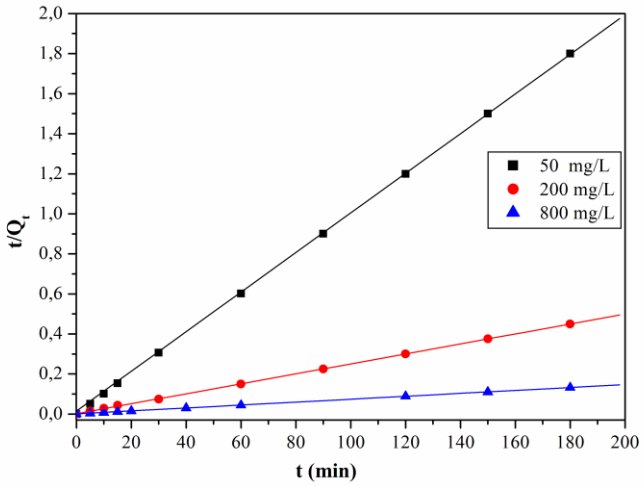

Figure 4: Pseudo-second order kinetic model for three different concentrations

The kinetic parameters are included in Table 2. According to Table 2, the values of the correlation coefficient are very close to unity for the three MO concentrations. This result is similar to that revealed in the literature confirming that the retention kinetics of several dyes is described by the pseudo-second model [27, 28]. In addition, the theoretical values of Q_e are close to the experimental values suggesting the conformity of this model [29].

Table 2: Parameters of the pseudo-second order kinetic model

Pseudo-second order					
C_0 (mg/L)	Equation t/Q_t =	k_2 (g/mg/h)	$Q_{e,\,th}$ (mg/g)	$Q_{e,\,exp}$ (mg/g)	R^2
50	0.0099×t + 0.0158	161.21	101.01	100.00	0.999
200	0.0025×t + 0.0018	288.00	400.00	399.87	1
800	0.0007×t + 0.0011	2244.89	1428.57	1346.96	0.999

3.5. Intraparticle diffusion mechanism

To interpret the interface phenomena that occur between the dye and the adsorbent material, it is necessary to exploit the intraparticle diffusion model in order to study its behavior and verify its contribution in the retention mechanism [30]; this model is presented in the following Equation (3):

$$Q_t = k_{id}\, t^{1/2} + C \quad (3)$$

Where Q_t is the amount of adsorption at the time t, k_{id} is the intraparticle diffusion rate constant (mg/g), and C is the vertical axis intercept, it is related to the thickness of the layer of the adsorbent which surrounds the particles of the adsorbate. The results of this model are presented in Figure 5.

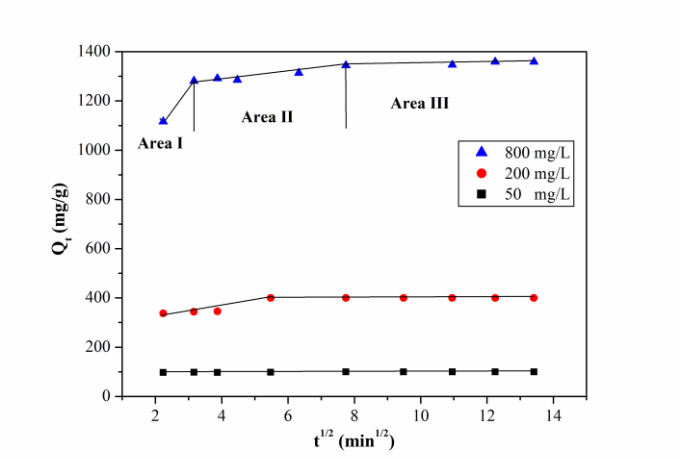

Figure 5: Linearized form of the intraparticle diffusion model

From this result, we can see three linearities for the highest concentration (800 mg/L). The area I complies to the adsorption of MO on the surface of CHT, but the area II concerns the intraparticle diffusion which can be explained by an intercalation of MO between the sheets of the reconstructed HT after rehydration. Finally, the area III is attributed to reach equilibrium state where all the material sites are occupied. These graphs can show a multilinearity indicating that two or more stages take place, the slowest step determines the overall rate of adsorption process [31, 32]. The constants for this model are illustrated in Table 3.

Table 3: Parameters for intraparticle diffusion of MO onto CHT

	Area I			Area II			Area III		
C_0 (mg/L)	k_{1d} (mg/g/$h^{1/2}$)	C_1 (mg/g)	R^2	k_{2d} (mg/g/$h^{1/2}$)	C_2 (mg/g)	R^2	k_{3d} (mg/g/$h^{1/2}$)	C_3 (mg/g)	R^2
50	0.262	96.95	0.907	-	-	-	-	-	-
200	19.49	284.95	0.923	-	-	-	0.016	399.70	0.821
800	177.91	718.82	1	13.374	1234.95	0.929	2.862	1320.60	0.890

3.6. Thermodynamic parameters of adsorption mechanism

The thermodynamic study was followed in the function of time inside a thermostatic bath, magnetically stirred charged with 1000 mg/L of aqueous MO solution in Erlenmeyer flask (100 mL), and hence the adsorbent was added to the solution with a mass of 30 mg. The study of the reaction environment temperature is highlighted at 298, 318 and 333 K with variable times between 15 and 210 min. The Gibbs free energy (ΔG°), was identified using the following Equation [33]:

$$\Delta G° = -RT\, LnK_d \quad (4)$$

The other parameters such as the entropy (ΔS°) and the enthalpy (ΔH°) were determined using the Van't Hoff equation:

$$LnK_d = \Delta S°/R - \Delta H°/RT \quad (5)$$

Where $K_d = Q_e/C_e$ is the distribution coefficient (L/g), R is the perfect gas constant and T is the temperature of the solution. The results are set out in Table 4. According to this study, it can be noted that the ΔH° value indicates an endothermic process. The ΔG° values confirms a spontaneous mechanism. ΔG° which decreases with temperature

suggests that the retention process is suitable when the temperature decreases [34]. In this case, ΔH° is equal to 0.666 kJ/mol, confirms a physically mechanism of MO adsorption by CHT [35-37]. The ΔS° value suggests randomness at the solid-solution interface [38]. The energy of activation gives additional information about the nature of process. It is linked to the second model rate constant (k_2) by the following Arrhenius relation:

$$Lnk_2 = LnA - E_a/RT \quad (6)$$

The obtained value for the activation energy which is 6.812 kJ/mol, indicates and confirms a physisorption mechanism [39].

Table 4: Thermodynamic parameters obtained by adsorption of MO on CHT at different temperatures

T (K)	E_a (kJ/mol)	Ln K_d	Q_e (mg/g)	ΔG° (kJ/mol)	ΔH° (kJ/mol)	ΔS° (J/mol.K)
298		2.011	2304.79	- 4.982		
318	6.812	2.023	2313.41	- 5.348	0.666	18.943
333		2.039	2325.26	- 5.647		

3.7. Isotherms of retention

Contact phenomenon between an adsorbent material and an adsorbate is generally evaluated by retention isotherms obtained from the determination of the adsorbed quantities and those remained in solution. The results of the retention of MO by CHT for three masses of 30, 50 and 80 mg, during 120 min of agitation at pH 6 as a function of the equilibrium concentration are plotted in Figure 6a. The linearized Langmuir isotherms plots are drawn in Figure 6b. The retention data of MO dye have been presented in accordance with the linear form of Langmuir Equation [40]:

$$C_e/Q = 1/(K.Q_m) + C_e/Q_m \quad (7)$$

Q is the quantity of MO retained by the unit mass of CHT (mg/g); Q_m, represents the maximum retained quantity of the dye; C_e, corresponds to the equilibrium concentration of MO (mg/L) and K is the affinity constant of MO for CHT (L/mg).

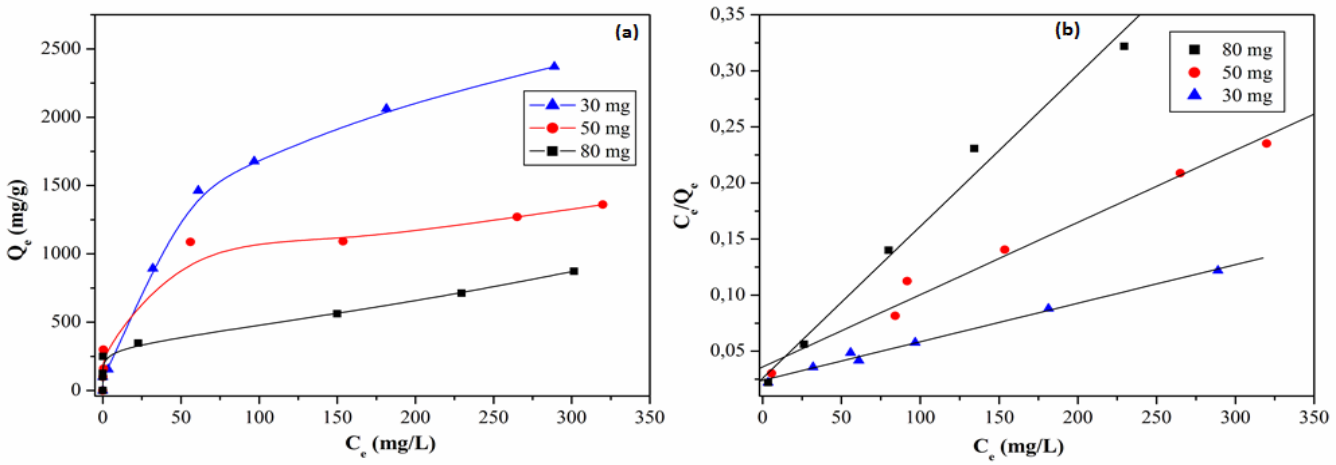

Figure 6: MO adsorption isotherms by CHT (a) and their linear forms according to the Langmuir model (b)

It is noted that the retention of MO is inversely proportional to the mass of CHT, and the shape of these isotherms is of L type according to the classification of Donohue and Aranovich [41]. This type of isotherm is consistent with a strong

attraction between the functional groups of the adsorbate and the adsorbent material, which suggests that the retention of the pollutant is probably achieved through the reconstruction of new HT phases [42]. The isotherms data need to fit precisely into different models to find an appropriate model that can be explored for the description of the retention process. According to the results given in Table 5, the adsorption of the dye MO is in good conformity with Langmuir model, following the value of the correlation coefficient R^2 which is close to unity. This model indicates that the retention is performed in monolayer [43].

Table 5: Parameter values of Langmuir adsorption isotherm model for MO on CHT

m_{CHT} (mg)	Q_m (mg/g)	K K (L/mg)	R^2
30	2500	0.024	0.962
50	1250	0.095	0.973
80	833.33	0.065	0.953

3.8. Effect of MO/CHT mass ratio

The adsorption capacity of the dye by CHT is influenced by the mass ratio adsorbate/adsorbent. These values are taken from the study of adsorption isotherms. It is noted that the retention is total when the mass ratio MO/CHT is between 0.1 and 0.3. To optimize the used amount of adsorbent, we must choose a ratio equal to 0.3 which represents a total elimination of the MO dye. The maximum retention capacity of MO by CHT reaches 2500 mg/g. The study of the influence of the mass of CHT on the adsorbed amounts of this pollutant is represented by the curve in Figure 7.

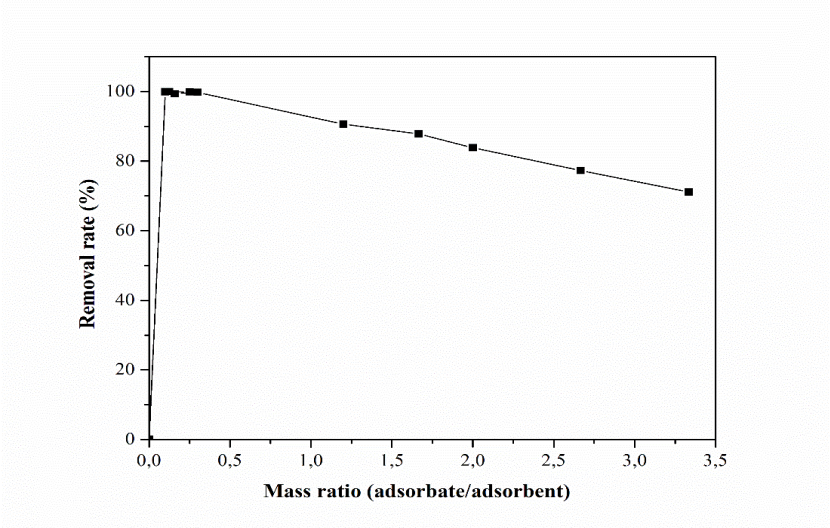

Figure 7: MO removal rate versus MO/CHT mass ratio

3.9. Characterizations after retention

3.9.1. XRD Analysis

The XRD result of the obtained phase after retention (Figure 8) indicates that it corresponds to a hydrotalcite type structure obtained by reconstruction. The shift of the line (003) appears at low value in 2 theta compared to that of the starting carbonated HT phase, indicates that the anions of the MO dye are intercalated between the HT sheets with an interlamellar distance of 2.35 nm. The appearance of a line around 61° confirms the reconstruction of the HT phase through the memory effect kept by the mixed oxides obtained after calcination at 500 °C (CHT). The lattice

parameters for this phase (HT-MO) intercalated by MO are: a = 0.306 nm, c = 7.05 nm and the interlamellar distance d = c/3 = 2.35 nm.

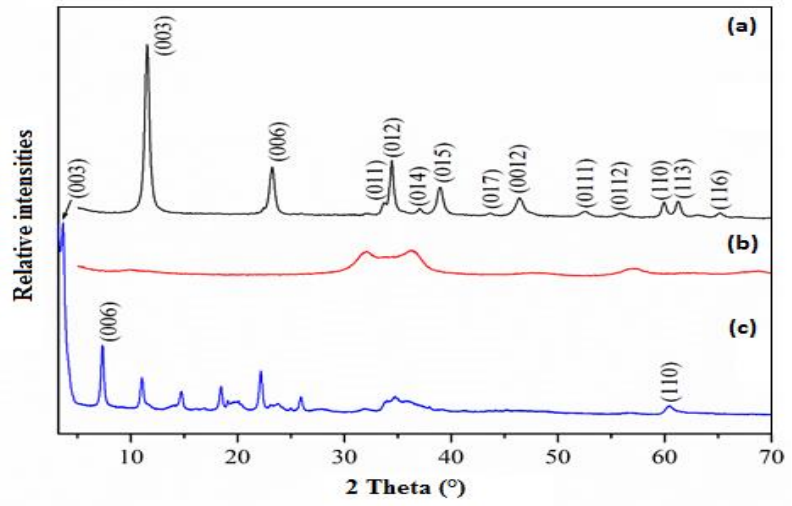

Figure 8: XRD patterns of the HT (a), CHT (b) phases and of the obtained phase HT-MO after retention of the MO dye (c)

3.9.2. IR Spectroscopy Analysis

This technique highlights the presence of the MO anions after their adsorption by the HT matrix. The IR spectrum of the phase obtained after MO retention is illustrated in Figure 9b. By comparison with the spectrum specific to MO (Figure 9c), we can point out the appearance of the characteristic bands of the dye. It shows symmetrical and antisymmetric C-H vibrations of (CH_3) located at 2854 and 2924 cm^{-1}. The C-C band corresponding to the benzene cycle vibration appears at 1542 and 1609 cm^{-1}. The vibration of N=N appears at 1421 cm^{-1} and the vibrations at 1369 and 1194 cm^{-1} are attributed to C-N. The asymmetric vibration of (S=O) is located around 1200 cm^{-1} and the symmetrical vibration of (S=O) is around 1050 cm^{-1}. The C-H vibrations of the benzene nucleus are located at 1039, 847, 818 and 698 cm^{-1} and those corresponding to C-S are observed around 700 cm^{-1}. We also note the presence of the C-H elongation bands around 600 and 550 cm^{-1} [44]. These results are in good agreement with those obtained by XRD, they confirm the presence of all the bands characteristic of the textile dye MO as well as the vibration bands characteristic of the reconstructed HT sheets around 430 and 638 cm^{-1}.

3.9.3. SEM-EDX Analysis

The image of the studied sample shows the appearance of crystallites of different sizes (Figure 10a), which come close to 1.3 µm. This result confirms that after retention of MO by CHT, there is indeed the appearance of a typical morphology of hydrotalcite which proves the reconstruction of an HT phase after rehydration. However, the presence of pollutant molecules on the surface causes a modification in the morphology due to the surface interactions between the CHT material and the dye, therefore influences the surface of the adsorbent material [45]. The EDX analysis of the reconstructed HT phase (Figure 10b) was carried out on separate points. We observe the appearance of emissions of zinc, aluminum, sulfur, oxygen, nitrogen and carbon which is mainly from benzene cycles, confirming the retention of the dye MO

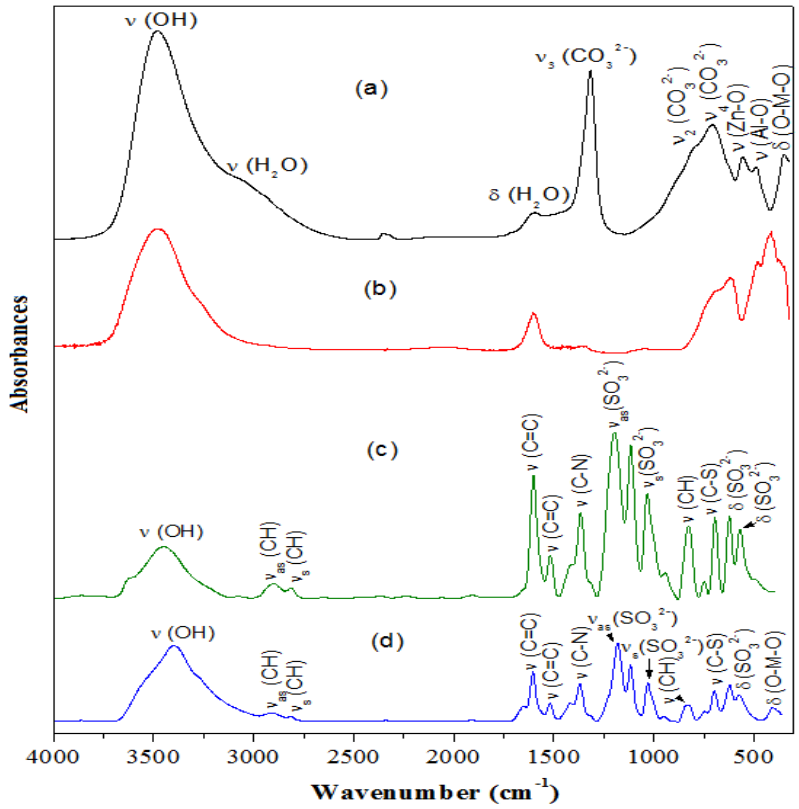

Figure 9: IR analysis of HT phase (a), calcined HT (b), MO dye (c) and HT-MO obtained after retention of MO (d)

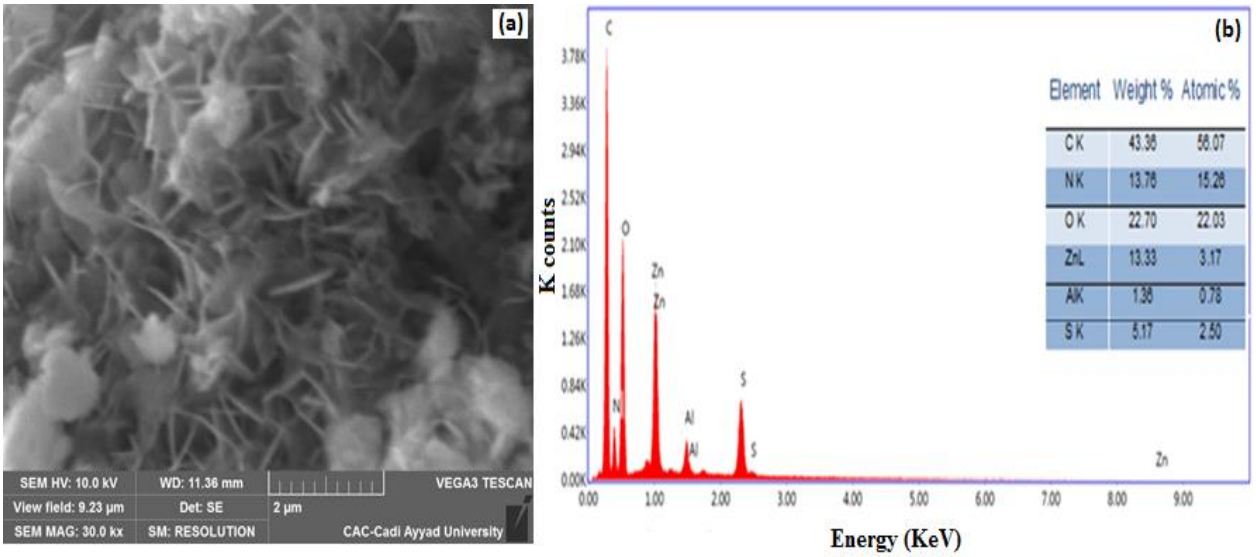

Figure 10: SEM photograph (a) and EDX analysis of the reconstructed phase HT-MO obtained after the retention of MO by CHT material (b)

3.10. Structural model

We have proposed a structural model which allows the arrangement, and proposes the orientation of the MO anion between the HT sheets after its retention. We have determined the length value of the MO molecule by the semi-

empirical molecular orbital method using Gaussian 03 Software. Figure 11 illustrates the orientation of the MO dye between the sheets of the reconstructed HT phase.

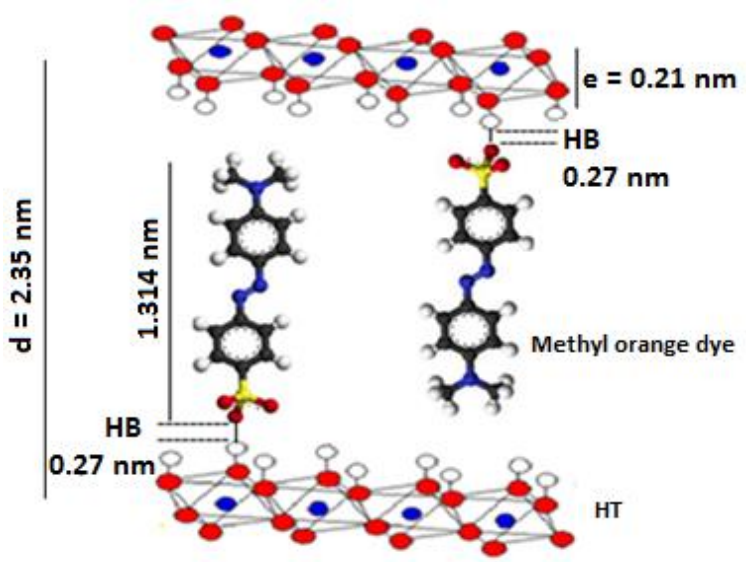

Figure 11: Structural model of MO orientation between HT sheets

The interlamellar distance determined experimentally is around 2.35 nm. The thickness of the HT sheet is 0.21 nm and the length of the hydrogen bond (HB) is 0.27 nm. The length of the molecule is 1.314 nm, comparable with the thickness of the gallery formed between the sheets after adsorption of MO. The latter is oriented vertically towards the hydroxyl plane by hydrogen bonds between the sulfonate groups SO_3^- of the dye and the hydroxyl groups OH of the reconstructed sheets, thus ensuring the adsorbate-adsorbent interaction [46].

3.11. Recycling tests of CHT

The main objective of CHT recycling is to explore the potential reuse of CHT as an adsorbent for MO from aqueous solutions. Thermal regeneration tests were carried out by calcining the synthesized adsorbent at 500 °C for 5 hours, followed by rehydration in a solution containing the MO anions. After this retention process the solid was recovered by filtration and dried, then impregnated with an excess of carbonate anions (CO_3^{2-}). The high affinity of the carbonate anions towards HT materials allows their intercalation in the interlayer space with an anionic exchange reaction of the pollutant. Recycling or regeneration takes place through a series of cycles, each of which includes calcination-rehydration-retention of polluting anions and their exchange by carbonate anions and then recalcination [47]. The process includes a series of five regeneration cycles. It is observed from these results that the fifth regeneration cycle have no significant effect on the retention capacity of the material. It can be noted that the elimination rate is only reduced to 94.54% after this process (Figure 12). This result suggests that the retention amount is affected by the CHT ability to regenerate a lamellar structure during the rehydration process. The MO removal rate is evaluated by the following Equation (8):

$$\% \text{ Removal rate} = (C_i - C_e)/C_i \times 100 \quad (8)$$

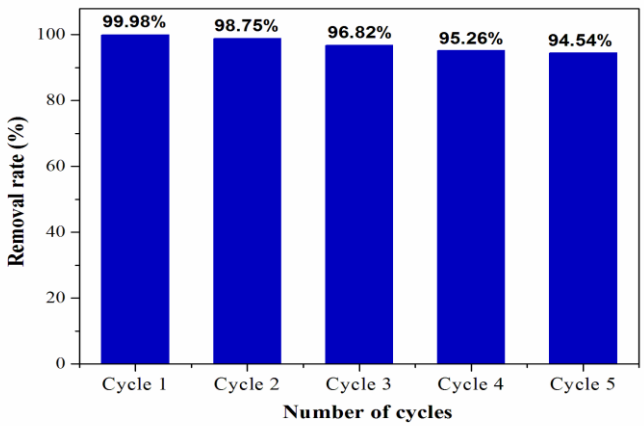

Figure 12: Recycling tests after MO removal by CHT material

According to this results, it can be concluded that the material CHT used provides that it has a relatively low cost and confirm his efficiency for the total removal of such pollutants. This recycling technique enabled us to recover the pollutants and wash waters for possible reuse.

3.12. Comparative study

In this paragraph we present the results of several researchers based on the retention of the MO dye by different materials. We will compare their retention capacities and elimination rates which are two indicators to assess the efficiency and the elimination power of such pollutants by CHT. The summary of the results is cited in Table 6.

Table 6: Maximum adsorption capacities and elimination rate of the MO dye by different materials

Adsorbents materials	Retention quantity (mg/g)	Removal rate (%)	References
Biomorph Mg-Al mixed metal oxides	182.8	99.72	[48]
Zeolite CuO/NaA	79.49	99	[49]
Biomass of chitosan	29	-	[50]
Nanocomposite γ-Fe_2O_3/2C	42.34	99.63	[51]
Zn-Al o mixed metal oxides	181.9	90.95	[43]
LDH MgNiAl	375	95	[52]
LDH NiAl	500.6	95	[53]
Cork powder	16.66	71.04	[54]
LDH NiFe	205.76	92	[55]
Zn-$AlNO_3$	2270.57	87	[56]
Mg-$AlNO_3$	1112.34	84	
Ni-$AlNO_3$	617.35	87	
Nanocomposite ZnO-Al_2O_3	291	97	[57]
CuS-NP-AC	122	99	[58]
Modified graphene oxide Ni-Cr LDH	312.5	95	[59]
Activated carbon prepared from *Vitis vinifera L.*	111.11	79.7	[60]
Superparamagnetic SiO_2/Fe_3O_4	240	100	[61]
Bimetal oxide/Graphene Gd_2O_3/Bi_2O_3/GO	544	95	[62]
Montmorillonite/Chitosan	1060	-	[63]
ZIF-67/CoAl-LDH	180.5	72.3	[64]
Calcined hydrotalcite	**2500**	**100**	**This work**

The calcined hydrotalcite used confirmed its efficiency. By comparing the retention capacities of the material used with those of other adsorbents, it can be concluded that it is competitive and promising for the treatment of wastewater.

4. Conclusion

The purpose of this study is achieved, the total retention of the azo dye MO from wastewater by CHT is studied, and the recycling performance of the adsorbent material is confirmed. Certain operating parameters have been optimized, such as the pH, the concentration of the adsorbate, the mass of the adsorbent material, the contact time and the temperature. According to this result, we affirm that the isotherms follow the Langmuir model, which means that there is a very high attraction between the adsorbate (MO) and the adsorbent (CHT). The maximum retention amount reaches 2500 mg/g with a total elimination (100%) for an optimal mass ratio (MO/CHT) of 0.3. The values of $\Delta H°$ and Ea suggest that the retention process of this pollutant is governed by a physisorption. Several analysis techniques have shown that the retention of this studied dye was achieved by a reconstruction of a hydrotalcite phase intercalated by the chosen textile dye. This study is a humble contribution to solving the problem of wastewater pollution caused by textile dyes in order to protect the quality of waters in particular and the environment in general.

References

[1] S. Dashamiri, M. Ghaedi, K. Dashtian, M.R. Rahimi, A. Goudarzi, R. Jannesar, Ultrason. Sonochem., 31 (2016) 546-557.

[2] A.S. Purnamo, V.T. Mauliddawati, M. Khoirudin, A.F. Yonda, R. Nawfa, S.R. Putra, Int. J. Environ. Sci. Technol., 16 (2019)7555-7564.

[3] A. Ammuri, S. Hejiouej, K. Ziat, M. Saidi, J. Mater. Environ. Sci., 5 (2014) 2066-2072.

[4] K.K.H. Choy, G. Mckay, J.F. Porter, Resour. Conserv. Recycl., 27 (1999) 57-71.

[5] N. Kannan, M. Meenakshisundaram, Water Air Soil Pollut., 138 (2001) 289-305.

[6] M. Shaban, M.R. Abukhadraa, A.A.P. Khan, B.M. Jibali, J. Taiwan Inst. Chem. Eng., 82 (2018) 102-~~1~~116.

[7] A.M. Awad, S.M.R. Sheikh, R. Jalab, M.H. Gulied, M.S. Nasser, A. Benamor, , S. Adham, Sep. Purif. Technol., 228 (2019) 115719.

[8] J. Kang, T.G. Levitskaia, S. Park, J. Kim, T. Varga, W. Um, Chem. Eng. J., 380 (2020) 122408.

[9] A. Zaher, M. Taha, A.A. Farghali, R.K. Mahmoud, Environ. Sci. Pollut. Res., 27 (2020) 12256-12269.

[10] E. H. Mourid, I. El Qor, L. Benaziz, M. Lakraimi, E. H. El Khattabi, Mor. J. Chem., 6(3) (2018) 425-433.

[11] T. Robinson, G. McMullan, R. Marchant, P. Nigam, Bioresour. Technol., 77 (2001) 247-255.

[12] G.Z. Kyzas, N.K. Lazaridis, A.C. Mitropoulos, Chem. Eng. J., 148 (2012) 189-190.

[13] M.T. Rahman, T. Kameda, T. Miura, S. Kumagai, T. Yoshioka, Chem. Ecol., 35 (2019) 128-142.

[14] S. Bouteraa, F. Boukraa, D. Saiah, S. Hamouda, N. Bettahar, Bull. Chem. React. Eng. Catal., 15 (2020) 43-54.

[15] E. Mourid, S. El Abridi, E. El Khattabi, M. Lakraimi, L. Benaziz, M. Berraho, Mor. J. Chem., 6(1) (2018) 122-134.

[16] M.A. El-Bindary, I.M. El-Deen, A.F. Shoair, J. Mater. Environ. Sci., 10 (2019) 604-617.

[17] S.M. Gidado, I. Akanyeti, Water Air Soil Pollut., 231 (2020) 146.

[18] M.A. Brown, S.C. Devito, Crit. Rev. Environ. Sci. Technol., 23 (1993) 249-324.

[19] S. Tsuda, N. Matsusaka, H. Madarame, S. Ueno, N. Susa, K. Ishida, N. Kawamura, K. Sekihashi, Y.F. Sasaki, Mutat. Res., 465 (2000) 11-26.
[20] B. Lellis, C. Z. Favaro-Polonio, J.A. Pamphile, J.C. Polonio, Biotechnol. Res. Innov., 3 (2019) 275-290.
[21] S.A. Misal, K.R. Gawai, Bioresour. Bioprocess., 5 (2018) 17.
[22] T. Kameda, M. Saito, Y. Umetsu, Mater. Trans., 47 (2006) 923-930.
[23] R. Alvarez, A. Toffolo, V. Pérez, C.F. Linares, Catal. Lett., 137 (2010) 150-155.
[24] H.C.B. Hansen, C.B. Koch, Appl. Clay Sci., 10 (1995) 5-19.
[25] N. Iyi, T. Matsumoto, Y. Kaneko, K. Kitamura, Chem. Mater., 16 (2004) 2926-2932.
[26] H.B. Yener, Chem. Biochem. Eng. Q., 33 (2019) 235-248.
[27] G.L. Dotto, L.A.A. Pinto, J. Hazard. Mater., 87 (2011) 164-170.
[28] S. Dawood, T.K. Sen, Water Res., 461 (2012) 1933-1946.
[29] K. Abdellaoui, I. Pavlovic, M. Bouhent, A. Benhamou, C. Barriga, Appl. Clay Sci., 143 (2017) 142-150.
[30] L. Mahardiani, A. Ashadi, S. Saputro, N.Y. Indriyanti, M. Taufiq, Mor. J. Chem., 8(4) (2020) 936-942.
[31] G. Crini, P.M. Badot, Prog. Polym. Sci., 33 (2008) 399-447.
[31] E. Mourid, M. Lakraimi, E. El Khattabi, L. Benaziz, M. Berraho, J. Mater. Environ. Sci., 8 (2017) 3121-3130.
[33] R. Lafi, A. Hafiane, J. Taiwan Inst. Chem. Eng., 58 (2016) 424-433.
[34] D.M. Mahmudunnabi, Md. Z. Alam, Md. Nurnabi, J. Mater. Environ. Sci., 11(4) (2020) 531-539.
[35] M. Alkan, O. Demirbas, S. Çelikçapa, M. Dogan, J. Hazard. Mater., B116 (2004) 135-145.
[36] D. Zhao, G. Sheng, J. Hu, C. Chen, X. Wang, Chem. Eng. J., 171 (2011) 167-174.
[37] A.A.A. Darwish, M. Rashad, H.A. AL-Aoh, Dyes Pigm., 160 (2019) 563-571.
[38] L. Lv, Desalination 208 (2007) 125-133.
[39] Y. Cantu, A. Remes, A. Reyna, D. Martinez, J. Villarreal, H. Ramos, S. Trevino, C. Tamez, A. Martinez, T. Eubanks, J.G. Parsons, Chem. Eng. J., 254 (2014) 374-383.
[40] I. Langmuir, J. Am. Chem. Soc., 40 (1918) 1361-1403.
[41] M.D. Donohue, G.L. Aranovich, J. Colloid Interface Sci., 205 (1998) 121-130.
[42] E. Mourid, M. Lakraimi, E. El Khattabi, L. Benaziz, M. Berraho, J. Mater. Environ. Sci., 8(3) (2017) 921-930.
[43] Z.M. Ni, S.J. Xia, L.G. Wang, F.F. Xing, G.X. Pan, J. Colloid Interface Sci., 316 (2007) 284-291.
[44] T. Shen, C. Jiang, C. Wang, J. Sun, X. Wang, X. Li, RSC Adv., 5 (2015) 58704-58712.
[45] F.P. De Sá, B.N. Cunha, L.M. Nunes, Chem. Eng. J., 215-216 (2013) 122-127.
[46] H. Laguna, S. Loera, I.A. Ibarra, E. Lima, M.A. Vera, V. Lara, Micropor. Mesopor. Mater., 98 (2007) 234-241.
[47] M. Hu, X. Yan, X.H u, R. Feng, M. Zhou, Colloids Surf. A Physicochem. Eng. Asp., 540 (2018) 207-214.
[48] L. Gao, Q. Li, X. Hu, X. Wang, H. Song, L. Yan, H. Xiao, Appl. Clay Sci., 126 (2016) 299-305.
[49] E.H. Mekatel, S. Amokrane, A. Aid, D. Nibou, M. Trari, C. R. Chim., 18 (2015) 336-344.
[50] F.N. Allouche, N. Yassaa, H. Lounici, Procedia Earth Planet. Sci., 15 (2015) 596-601.
[51] R. Istratie, M. Stoia, C. Pacurariu, C. Locovei, Arab. J. Chem., 12 (2019) 3704-3722.
[52] H. Zaghouane-Boudiaf, M. Boutahala, L. Arab, Chem. Eng. J., 187 (2012) 142-149.
[53] K. El Hassani, B.H. Beakou, D. Kalnina, E. Oukani, A. Anouar, Appl. Clay Sci., 140 (2017) 124-131.
[54] F. Krika, O.F. Benlahbib, Desalin. Water Treat., 53 (2015) 3711-3723.
[55] Y. Lu, B. Jiang, L. Fang, F. Ling, J. Gao, F. Wu, X. Zhang, Chemosphere 152 (2016) 415-422.
[56] F.Z. Mahjoubi, A. Elhalil, R. Elmoubarki, M. Sadiq, A. Khalidi, O. Cherkaoui, N. Barka, J. Appl. Surf. Interfaces, 2 (2017) 1-11.

[57] H. Tajizadegan, O. Torabi, A. Heidary, M.H. Golabgir, A. Jamshidi, Desalin. Water Treat., 57 (2016) 12324-12334.
[58] P. Mokhtari, M. Ghaedi, K. Dashtian, M.R. Rahimi, M.K. Purkait, J. Mol. Liq., 219 (2016) 299-305.
[59] X. Ruan, Y. Chen, H. Chen, G. Qian, R.L. Frost, Chem. Eng. J., 297 (2016) 295-303.
[60] V. Yönten, N.K. Sanyürek, M.R. Kivanç, Surf. Interfaces, 20 (2020) 100529.
[61] A. Gallo-Cordova, J. Lemus, F.J. Palomares, M.P. Morales, E. Mazario, Sci. Total Environ., 711 (2020) 134644.
[62] T.R. Das, P.K. Sharma, Mater. Sci. Semicond. Process., 105 (2020) 104721.
[63] S. Kang, L. Qin, Y. Zhao, W. Wang, T. Zhang, L. Yang, F. Rao, S. Song, Chemosphere 238 (2020) 124693.
[64] M.A. Nazir, N.A. Khan, C. Cheng, S.S.A. Shah,T. Najam, M. Arshad, A. Sharif, S. Akhtar, A. ur Rehman, Appl. Clay Sci., 190 (2020) 105564.